18th Brazilian Congress of Thermal Sciences and Engineering
November 16-20, 2020 (Online)

ENC-2020-0332
SUPERCRITICAL FLUID EXTRACTION: BRANCHED PORE MODEL WITH NON-LINEAR EQUILIBRIUM

Augusto Cezar Cordeiro Jardim
Diego Sousa Lopes
Graduate Program in Chemical Engineering, Federal University of Pará
augustojardim@gmail.com, diegosousa.eng@gmail.com

Josiel Lobato Ferreira
School of Chemical Engineering, Federal University of Pará
jlobato@ufpa.br

Raul Nunes de Carvalho Júnior
School of Food Engineering, Federal University of Pará
raulncj@ufpa.br

Diego Cardoso Estumano
School of Biotechnology, Federal University of Pará
dcestumano@ufpa.br

Emanuel Negrão Macêdo
João Nazareno Nonato Quaresma
School of Food Engineering, Graduate Program in Chemical Engineering, Graduate Program in Process Engineering, Graduate Program in Natural Resources Engineering in the Amazon, Federal University of Pará
enegrao@ufpa.br, quaresma@ufpa.br

Abstract. *A mathematical model was proposed in the present work to describe the supercritical fluid extraction. He started from the material differential balances of the fluid and the particle and introduced the idea of branched pores; the method of lines (MOL) was used to solve this model. The system of ordinary differential equations resulting from the application of the numerical method was solved with the aid of a computational code developed in FORTRAN programming language using the DIVPAG routine from the IMSL library. The effects of temperature were evaluated for the extraction of priprioca (Cyperus articulatus) and ucuuba (Virola surinamensis Warb.) oils; the effects of pressure were evaluated to extract black sesame (Sesamum indicum) seed and priprioca oils. The results obtained were compared to those in the literature for the model validation and they had an excellent agreement with experimental data.*

Keywords: *supercritical fluid extraction, priprioca, ucuuba and black sesame seed oils, method of lines*

1. INTRODUCTION

Supercritical fluid extraction is considered a non-conventional technique of advanced separation based on the solvation power of fluids and high selectivity. The main characteristic of this extraction is the use of solvents at temperatures more significant than its critic temperature and pressure higher than critic pressure, i.e., solvents at their supercritical state (Ruslan et al., 2018; Hernandez et al., 2019).

The use of this technique of extraction brings some advantages: good qualitative and quantitative yields; conservation of the material avoid oxidation and degradation; the possibility of reuse and recovery of used solvent; lower energy expenditure in comparison to distillation; the higher speed of processing due to fluid characteristics (high diffusivity, low viscosity, and adequate solvation power) (Santos and Lannes, 2015).

Nevertheless, the process presents some disadvantages and limitations that could be bypassed or that end up being compensated. An example of this is the high initial investment value that becomes an obstacle to industrial spread (Santos, 2011). Despite that, this cost is compensated since the operation cost is lower than that of other extraction techniques, so the total expenses equate when the process is optimized (Santos, 2012).

Another drawback is the difficulty in extracting polar compounds from the solid matrix, which happens due to the apolar character of the fluid utilized (usually CO2). The addition of modifiers or cosolvents could overcome this drawback (Costa, 2015).

The potential of supercritical fluid extraction applications is vast and can be employed in a wide range of industries since the food industry until chemical processing and energy industries.

Some utilizations of supercritical fluid extraction in food and beverage industries can include: the decaffeination of coffee and of black tea, extraction of compounds of hop and spices, obtainment of essential oils of aromatic herbs, to be utilized as preservatives in meat products, are some of the utilizations of supercritical fluid extraction in food and beverage industries (Knez et al., 2014; Tomovic et al., 2019). In the cosmetic and pharmaceutical industries, this technique of extraction is employed to obtain phenolic compounds that present a broad spectrum of biological properties like antioxidants, antibiotics, anti-inflammatory, etc. (Tyśkiewicz et al., 2018; Yousefi et al., 2019).

In the fuel industry, uses can be the desulfurization of mineral coal, the recovery of liquid fuels from lignite coal, the production of gaseous fuels (hydrogen and carbon monoxide) from bitumen, and the obtainment of liquid and gaseous fuels from shale oil (Marcus, 2019).

Recent works have demonstrated the feasibility of using supercritical fluid extraction: for the recovery of rare elements earth existent in nickel-metal hydride battery (Ni-MH) from hybrid electric cars (Yao et al., 2017); and the removal of cesium in contaminated soil (Leybros et al., 2016).

Supercritical fluid extraction has substantial advantages, high applicability, few limitations, and it is technically feasible. However, it is disregarded compared to other techniques of separation solid-fluid due to its high initial investment cost. In this context, it is necessary to obtain a means to assess the process's economic viability. Therefore, it is essential to propose mathematical models to evaluate process parameters through simulations and use such models for process design (Jesus, 2015).

Mathematical models are formulations that simulate the dynamics of state variables, in which it is possible to measure one of these variables. The objective of mathematical modeling is to reproduce experimental data, using hypotheses. These hypotheses are based on transport phenomena theories of supercritical fluid extraction, or an empirical basis, and are useful utilities in the study of scale-up and implementation of industries.

Mathematical models of supercritical fluid extraction are based on the mass balance in the fluid and solid phases. The mass balance in the fluid phase in models present in the literature tends to be similar. However, when observing the mass balance in the solid phase, marked differences arise since each author will use his simplifying assumptions and consider the composition of the solid matrix (Oliveira et al., 2011).

The differences mentioned above are evident in three of the main extraction models: the broken and intact cells (BIC) model proposed by Sovová (1994) that considers the existence of cells inside the solid matrix that holds the solute. These cells are divided into intact and broken since it is regarded as a grinding process before extraction; the easily accessible solute is located in the damaged cells, and the hard-to-reach solute is found in the intact cells. The shrinking core model proposed by Goto et al. (1996) assumes that the solute is present within the core of the porous matrix, and as the extraction proceeds, the body shrinks. The hot ball model treats the extraction of solute from the solid matrix as a hot ball cooling in a uniform medium (Reverchon et al., 1993).

In this work, a mathematical model is proposed to simulate the supercritical fluid extraction process predicting the behavior of its kinetic curve. This novel model considers the existence of macropores and micropores simultaneously inside the solid matrix. The proposed model is solved using the method of lines (MOL), and experimental data from literature were used for validation.

2. MATHEMATICAL FORMULATION

The mathematical model proposed is based on differential mass balances in the fluid and solid phases and takes into account the mass transfer and the interaction solute-solid. Besides that, introduce the idea of branched pores in supercritical fluid extraction systems: pores that are divided into regions of macropores and micropores, being the last branches of the macropore network. Peel et al. (1981) state that in the macropore region occurs a rapid diffusion and adsorption of the fluid in the solid matrix, while in the micropore region, there is a slower transport that leads to the equilibrium.

It is relevant to point out that the proposed model is valid to a solid matrix with microporous crystals. Also, the following simplifying assumptions were adopted to the model formulation:

1. The solid matrix is porous and has macropores and micropores;
2. The oil is evenly distributed;
3. The porous array is spherical and uniform;
4. The mass transfer is one-dimensional and transient in the bed;
5. The mass transfer is one-dimensional and unsteady in the particle;
6. The equilibrium inside the particle occurs nonlinearly, and the Langmuir isotherm is used to describe this equilibrium;
7. The flow is axially dispersed and without radial dispersion;

8. The solute is considered a single chemical component;
9. The system is isothermal and isobaric;
10. The flow rate is uniform;
11. The control volume is large enough that: $(\partial Caf/\partial z)_{z=L} = 0$.

Based on molar balances in the bed, which considers diffusive and convective transports, mass transfer resistance and the assumptions adopted, the following mathematical model with their respective initial condition and boundary conditions was proposed to describe a supercritical fluid extraction process:

$$\frac{\partial Caf}{\partial t} + u_o \frac{\partial Caf}{\partial z} = Dax \frac{\partial^2 Caf}{\partial z^2} - \frac{(1-\varepsilon_l)}{\varepsilon_l} a_f K_f \left(Caf - Cap\big|_{Rp} \right);\ t>0;\ 0<z<L \tag{1}$$

$$E_d \frac{\partial Cap}{\partial t} = \frac{1}{r^2}\frac{\partial}{\partial r}\left(r^2 Def \frac{\partial Cap}{\partial r} \right);\ t>0;\ 0<r<Rp \tag{2}$$

$$Caf = Caf_0 \quad for \quad t=0 \tag{3}$$

$$Cap = Cap_0 \quad for \quad t=0 \tag{4}$$

$$Dax \frac{\partial Caf}{\partial z} = u_0 (Caf - Cae) \quad at \quad z=0 \tag{5}$$

$$\frac{\partial Caf}{\partial z} = 0 \quad at \quad z=L \tag{6}$$

$$\frac{\partial Cap}{\partial r} = 0 \quad at \quad r=0 \tag{7}$$

$$Def \frac{\partial Cap}{\partial r} = K_f (Caf - Cap) \quad at \quad r=Rp \tag{8}$$

where,

$$E_d = \varepsilon_p + (1-\varepsilon_p)\rho_p f(Cap) \tag{9}$$

$$Def = \varepsilon_p D_{mac} + (1-\varepsilon_p)\rho_p D_{mic} f(Cap) \tag{10}$$

$$f(Cap) = \frac{q_{máx} b}{(1+bCap)^2} = \frac{K}{(1+bCap)^2} \tag{11}$$

In which Caf is the solute concentration in the fluid phase (kg/m³); Cap is the solute concentration in the volume of macropores (kg/m³); Cae is the solute concentration in the fluid phase at z=0 (kg/m³); t is the time (s); z is the axial coordinate (m); r is the radial coordinate (m); a_f is the specific surface of the solid (m^{-1}); Dax is the axial dispersion coefficient (m²/s); D_{mac} is the diffusivity in the macropores (m²/s); D_{mic} is the diffusivity in the micropores (m²/s); Def is the effective diffusivity (m²/s); u_o is the interstitial velocity (m/s); K_f is the mass transfer coefficient; $q_{máx}$ is the maximum adsorption capacity (kg/kg); b is the Langmuir affinity constant (m³/kg); $f(Cap)$ is a relationship that comes from the law (Langmuir) that governs the equilibrium within the particle; ε_l is the void fraction of the bed; ε_p is the porosity of the particles.

In Eq. (1) the term $\partial Caf/\partial t$ represents the rate of solute accumulation within the fluid; the term $u_0 \partial Caf/\partial z$ the solute transport by convection; the term $Dax\partial^2 Caf/\partial z^2$ the solute transport by diffusion and the term $[(1-\varepsilon_l)/\varepsilon_l]a_f K_f(Caf - Cap|_{Rp})$ the transport of solute from the particle surface to the fluid phase and considers the resistance to mass transfer in the outer film that forms around the particle.

In Eq. (2) the term $E_d \partial Cap/\partial t$ express the accumulation of solute in the particles and the term $(1/r^2)\partial(r^2 Def \partial Cap/\partial r)/\partial r$ describes the diffusion within the particle, i.e. the diffusion in macropores and micropores.

Equations (5) and (6) are boundary conditions related to equation (1) and are the same proposed by Danckwertz (1953). Equation (7) is the symmetry condition, and Eq. (8) is the boundary condition fror Eq. (2).

It is useful and necessary to write Eqs. (1) to (11) in dimensionless form. For this purpose, the dimensionless groups are defined below:

$$Y = \frac{Caf}{Cap_o};\ X = \frac{Cap}{Cap_o};\ Y_e = \frac{Cae}{Cap_o};\ Y_o = \frac{Caf_o}{Cap_o};\ Z = \frac{z}{L};\ \eta = \frac{r}{Rp} \tag{12-17}$$

$$\tau = \frac{u_0 t}{L};\ W = \frac{a_f K_f L}{u_0};\ Pe = \frac{u_0 L}{Dax};\ a = \frac{L D_{mac}}{Rp^2 u_0};\ \tilde{D}ef = \frac{Def}{D_{mac}} \tag{18-22}$$

$$d = \frac{D_{mic}}{D_{mac}};\ \gamma = bCap_o;\ Bim = \frac{K_f Rp}{D_{mac}};\ \beta = \rho_p K.d \tag{23-26}$$

Then, the dimensionless mathematical formulation is written as:

$$\frac{\partial Y}{\partial \tau} + \frac{\partial Y}{\partial Z} = \frac{1}{P_e}\frac{\partial^2 Y}{\partial Z^2} - \frac{(1-\varepsilon_l)}{\varepsilon_l} W\left(Y - X\big|_{\eta=1}\right);\ \tau > 0;\ 0 < Z < 1 \tag{27}$$

$$\tilde{E}_d \frac{\partial X}{\partial \tau} = \frac{a}{\eta^2}\frac{\partial}{\partial \eta}\left(\eta^2 \tilde{D}ef \frac{\partial X}{\partial \eta}\right);\ \tau > 0;\ 0 < \eta < 1 \tag{28}$$

$$Y = Y_0 \quad for \quad \tau = 0 \tag{29}$$

$$X = 1 \quad for \quad \tau = 0 \tag{30}$$

$$-\frac{\partial Y}{\partial Z} = Pe(Y_e - Y) \quad at \quad Z = 0 \tag{31}$$

$$\frac{\partial Y}{\partial Z} = 0 \quad at \quad Z = 1 \tag{32}$$

$$\frac{\partial X}{\partial \eta} = 0 \quad at \quad \eta = 0 \tag{33}$$

$$\tilde{D}ef \frac{\partial X}{\partial \eta} = Bim(Y - X) \quad at \quad \eta = 1 \tag{34}$$

where,

$$\tilde{E}_d = \varepsilon_p + \left(1 - \varepsilon_p\right)\frac{\beta}{\left(1+\gamma X\right)^2}\frac{1}{d} \tag{35}$$

$$\tilde{D}ef = \varepsilon_p + \left(1 - \varepsilon_p\right)\frac{\beta}{\left(1+\gamma X\right)^2} \tag{36}$$

The computation of the extracted mass was evaluated from the following equations:

$$E = \int_0^\tau Q_{massa}\, Y\big|_{Z=1}\, d\tau \tag{37}$$

$$Q_{massa} = \frac{Q_{fs} LCap_o}{u_o} \tag{38}$$

Where Q_{fs} is volumetric flow of supercritical fluid.

The extraction yields are made using the following formulations:

$$Yield\ (\%) = \frac{mass\ of\ solute\ extracted}{solid\ matrix\ mass} \times 100 \tag{39}$$

$$dry\ basis\ yield\ (\%) = \frac{mass\ of\ solute\ extracted}{solid\ matrix\ mass \times \left(\frac{100-U}{100}\right)} \times 100 \tag{40}$$

In which U is the percentage of humidity of the solid matrix.

3. SOLUTION METHODOLOGY

The dimensionless model was solved applying the method of lines (MOL), which is a numerical technique adopted to solve partial differential equations (PDEs).

Basically, the method involves approximation by finite differences (or finite volumes) of all spatial differential operators, this means that the original partial differential equation (PDE) and its boundary conditions will be transformed into a system of ordinary differential equations (ODEs) as an initial value problem in the time variable

(OZISIK et al., 2017). In other words, the spatial differential operators will be replaced by a formula of finite differences keeping only one independent variable.

The axial variable is divided into intervals. The derivatives are approximated by finite differences for the nodes $1 \leq i \leq NIZ\text{-}1$. Thus, Eqs. (27), (29), (31) and (32) become:

$$\frac{dY_i}{d\tau} = \delta_i - \Gamma_i - \frac{(1-\varepsilon_l)}{\varepsilon_l} W\left(Y_i - X_{i,Ni\eta}\right);\ 1 \leq i \leq NIZ-1 \tag{41}$$

$$Y_i = Y_0;\ \tau = 0 \tag{42}$$

$$Y_0 = \frac{2\Delta ZPeY_e + 4Y_1 - Y_2}{3 + 2\Delta ZPe};\ i=0 \tag{43}$$

$$Y_{NIZ} = \frac{4Y_{NIZ-1} - Y_{NIZ-2}}{3};\ i = NIZ \tag{44}$$

where,

$$\Gamma_i = \left.\frac{\partial Y}{\partial Z}\right|_i = \frac{Y_i - Y_{i-1}}{\Delta Z} \tag{45}$$

$$\delta_i = \frac{1}{Pe}\frac{\partial^2 Y}{\partial Z^2} = \frac{Y_{i+1} - 2Y_i + Y_{i-1}}{Pe\Delta Z^2} \tag{46}$$

In a similar way, the radial variable is also divided in intervals. The derivatives are approximated by finite differences for the nodes $1 \leq j \leq NI\eta\text{-}1$. Therefore, Eqs. (28), (30), (33) and (34) become:

$$\tilde{E}_{dj}\frac{dX_j}{d\tau} = \lambda_j;\ 1 \leq j \leq NI\eta - 1 \tag{47}$$

$$X_j = 1;\ \tau = 0 \tag{48}$$

$$X_0 = \frac{4X_1 - X_2}{3};\ j = 0 \tag{49}$$

$$\tilde{Def}\left(\frac{X_{NI\eta-2} - 4X_{NI\eta+1} + 3X_{NI\eta}}{2\Delta\eta}\right) = Bim\left(Y_i - X\big|_{NI\eta}\right);\ j = 1 \tag{50}$$

where,

$$\tilde{E}_{dj} = \varepsilon_p + \left(1-\varepsilon_p\right)\frac{\beta}{\left(1+\gamma X_j\right)^2}\frac{1}{d} \tag{51}$$

$$\lambda_j = \frac{a}{\eta^2}\left[2\eta\tilde{Def}\left(\frac{X_{j+1} - X_{j-1}}{2\Delta\eta}\right) + \eta^2\frac{\partial\tilde{Def}}{\partial X}\left(\frac{X_{j+1} - X_{j-1}}{2\Delta\eta}\right)^2 + \eta^2\tilde{Def}\left(\frac{X_{j+1} - 2X_j + X_{j-1}}{\Delta\eta^2}\right)\right] \tag{52}$$

$$\tilde{Def} = \varepsilon_p + \left(1-\varepsilon_p\right)\frac{\beta}{\left(1+\gamma X_j\right)^2} \tag{53}$$

Equation (50) can be manipulated and becomes an equation that has three roots. With the aid of the software of symbolic computation *Mathematica*, we obtain the three solutions, of which two are complex and only one is real, we discard the complex ones and use the real solution shown below:

$$X_{i,NI\eta} = \frac{-B}{3A} + \frac{\sqrt[3]{2}E}{3A\left(-F + \sqrt{-4E^3 + F^2}\right)^{1/3}} + \frac{\left(-F + \sqrt{-4E + F^2}\right)^{1/3}}{3A\sqrt[3]{2}} \tag{54}$$

$$A = 2Bim\gamma^2\Delta\eta;\quad B = 4Bim\gamma\Delta\eta - AY_i;\quad C = 3\beta + 2Bim\Delta\eta - 4Bim\Delta\eta\gamma Y_i \tag{55-57}$$

$$D = \beta X_{i,NI\eta-2} - 4\beta X_{i,NI\eta-1} - 2Bim\Delta\eta Y_i;\quad E = B^2 - 3AC;\quad F = 2B^3 - 9ABC + 27A^2D \tag{58-60}$$

The resulting system of ODEs and the respective initial conditions are:

$$\frac{dY_i}{d\tau} = \delta_i - \Gamma_i - \frac{(1-\varepsilon_l)}{\varepsilon_l} W\left(Y_i - X_{i,Ni\eta}\right);\ \tau > 0 \text{ and } 1 \le i \le NIZ-1 \tag{61}$$

$$\tilde{E}_{di,j}\frac{dX_{i,j}}{d\tau} = \lambda_{i,j};\ \tau > 0 \text{ and } 1 \le j \le NI\eta - 1 \tag{62}$$

$$Y_i = Y_0;\ \tau = 0; \quad X_{i,j} = 1;\ \tau = 0 \tag{63,64}$$

$$Y_0 = \frac{2\Delta ZPeY_e + 4Y_1 - Y_2}{3 + 2\Delta ZPe};\ i=0; \quad Y_{NIZ} = \frac{4Y_{NIZ-1} - Y_{NIZ-2}}{3};\ i = NIZ \tag{65,66}$$

$$X_0 = \frac{4X_1 - X_2}{3};\ j = 0; \quad X_{i,NI\eta} = \frac{-B}{3A} + \frac{\sqrt[3]{2}E}{3A\left(-F + \sqrt{-4E^3 + F^2}\right)^{1/3}} + \frac{\left(-F + \sqrt{-4E + F^2}\right)^{1/3}}{3A\sqrt[3]{2}};\ j = NI\eta \tag{67,68}$$

This system of ODEs was numerically solved by the DIVPAG routine from the IMSL Library in FORTRAN 90/95 programming language. The DIVPAG routine utilized Adams-Moulton method with an error prescribed of 10^{-8} by the user.

4. RESULTS AND DISCUSSION

In order to validate the proposed model nine cases were studied. Experimental data of three different solid matrices were obtained from the literature.

Table 1 present the type of solid matrix, temperature and pressure, as well as the authors who published the data used for the validation of the model. The cases 1, 2, 3 and 4 were used to study the effect of temperature in supercritical fluid extraction (SFE); the cases 5, 6, 7 and 8 were utilized to study the effect of pressure in SFE.

Table 1. Operational conditions of cases to study effect of temperature and pressure.

Case	Solid matrix	Temperature (K)	Pressure (MPa)	Author/year
1	Ucuuba	313	35	Cordeiro et al. (2018)
2	Ucuuba	353	35	Cordeiro et al. (2018)
3	Priprioca	313	25	Silva et al. (2014)
4	Priprioca	323	25	Silva et al. (2014)
5	Priprioca	333	25	Silva et al. (2014)
6	Priprioca	333	13	Silva et al. (2014)
7	Black Sesame Seed	333	20	Botelho et al. (2014)
8	Black Sesame Seed	333	40	Botelho et al. (2014)

The values of the dimensionless parameters a, β, Bim, d, γ, Pe and W, were optimized according to the trial and error procedure, always observing the behavior of the extraction curves for a better approximation of the experimental data. Table 2 shows these values.

Table 2. Values of the dimensionless parameters.

Parameters/Cases	Case 1	Case 2	Case 3	Case 4	Case 5	Case 6	Case 7	Case 8
a	$6.67\text{x}10^{4}$	$3.36\text{x}10^{4}$	$7.62\text{x}10^{2}$	$4.20\text{x}10^{2}$	$1.68\text{x}10^{2}$	$1.50\text{x}10^{1}$	$7.78\text{x}10^{-3}$	$6.29\text{x}10^{2}$
β	$6.13\text{x}10^{-1}$	$6.62\text{x}10^{-1}$	$1.61\text{x}10^{-2}$	$1.60\text{x}10^{-2}$	$1.65\text{x}10^{-2}$	$4.28\text{x}10^{-3}$	$9.28\text{x}10^{-2}$	$9.16\text{x}10^{-3}$
Bim	$3.37\text{x}10^{-1}$	$4.11\text{x}10^{-1}$	$5.44\text{x}10^{1}$	$7.63\text{x}10^{1}$	$1.20\text{x}10^{2}$	$3.15\text{x}10^{2}$	$1.25\text{x}10^{6}$	3.15
d	$2.6\text{x}10^{-2}$	$1.8\text{x}10^{-2}$	$8.13\text{x}10^{-4}$	$8.2\text{x}10^{-4}$	$8.33\text{x}10^{-4}$	$5.30\text{x}10^{-5}$	$6.00\text{x}10^{-4}$	$1.72\text{x}10^{-5}$
γ	$4.93\text{x}10^{-1}$	$9.86\text{x}10^{-1}$	$5.43\text{x}10^{-3}$	$6.71\text{x}10^{-3}$	$4.45\text{x}10^{-2}$	$1.33\text{x}10^{-3}$	7.39	2.46
Pe	1.54	2.62	1.16	1.80	3.75	$4.61\text{x}10^{1}$	3.22	$1.59\text{x}10^{1}$
W	$6.74\text{x}10^{4}$	$4.14\text{x}10^{4}$	$1.24\text{x}10^{5}$	$9.60\text{x}10^{4}$	$6.06\text{x}10^{4}$	$1.42\text{x}10^{4}$	$2.93\text{x}10^{4}$	$5.95\text{x}10^{3}$

Mesh convergence analyzes were performed on the ODEs system solutions, one for each solid matrix. Tables 3, 4, and 5 present the axial and radial mesh convergence results for solute concentration in the fluid at the end of time and two different positions in the extractor (Z=1/3 and Z=1 for the priprioca oil, and Z=0.3 and Z=1 for the other solid matrices). Three significant digits were adopted to analyze priprioca and ucuuba, while two were used for black sesame.

The results allow us to affirm that the convergence was reached in the axial coordinate in 240, 90, and 180 intervals. The radial coordinate was achieved in 15, 35, and 10 intervals for priprioca, black sesame, and ucuuba.

Table 3. Convergence for the concentration of solute in the fluid for the extraction of priprioca oil.

	Z=1/3	**Z=1**	**Z=1/3**	**Z=1**	**Z=1/3**	**Z=1**
NIZ/NIη	**10**	**10**	**15**	**15**	**20**	**20**
210	0.893	1.2126	0.8928	1.2124	0.8929	1.2124
240	0.8934	1.2133	0.8934	1.2132	0.8932	1.2130
270	0.8938	1.2138	0.8938	1.2137	0.8937	1.2136

Table 4. Convergence for the concentration of solute in the fluid for the extraction of black sesame.

	Z=0.3	**Z=1**	**Z=0.3**	**Z=1**	**Z=0.3**	**Z=1**
NIZ/ NIη	**30**	**30**	**35**	**35**	**40**	**40**
60	0.5971	1.0081	0.5957	1.0058	0.5947	1.0043
90	0.5980	1.0107	0.5966	1.0084	0.5956	1.0069
120	0.5985	1.0120	0.5970	1.0098	0.5961	1.0082

Table 5. Convergence for the concentration of solute in the fluid for the extraction of ucuuba oil.

	Z=0.3	**Z=1**	**Z=0.3**	**Z=1**	**Z=0.3**	**Z=1**
NIZ/ NIη	**5**	**5**	**10**	**10**	**15**	**15**
150	0.04701	0.06907	0.04696	0.06898	0.04696	0.06899
180	0.04712	0.06923	0.04705	0.06912	0.04705	0.06912
210	0.04717	0.06931	0.04712	0.06923	0.04712	0.06923

4.1 Influence of temperature on the extraction of ucuuba oil and priprioca oil

In Fig. 1, it can be seen that an increase in temperature at constant pressure increases the yield of ucuuba oil extraction. Similarly, in Fig.2, it can be observed that an increase in temperature under a stable pressure raises the cumulative amount extracted of priprioca oil. It is necessary to note two mechanisms that occur when the temperature is raised at constant pressure to understand this behavior. First, the decrease of the fluid density and its solvation power leads to a reduction in the yield and cumulative amount extracted. Second, the increase in the solute's vapor pressure leads to an augmentation in yield and mass of solute extracted. These two mechanisms are antagonistic, and one of them is dominant. Due to the comportment of the extraction curves, it can be concluded that the increase in the solute vapor pressure is the dominant mechanism.

The proposed model was able to represent the experimental data of the solid matrices satisfactorily.

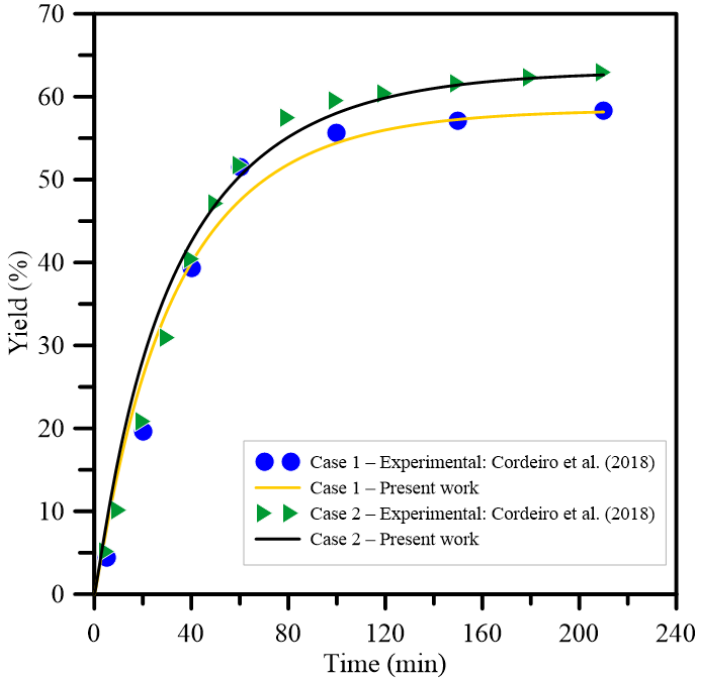

Figure 1. Effect of the temperature on the extraction of ucuuba oil.

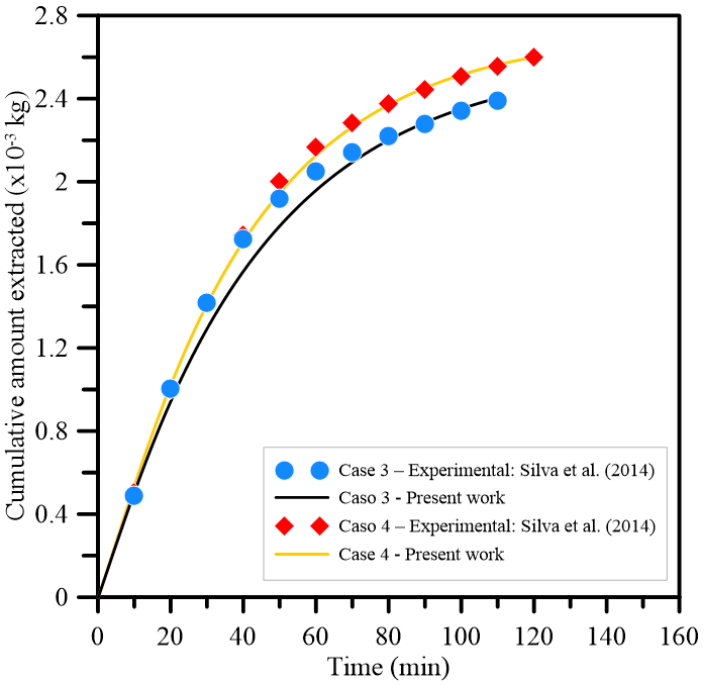

Figure 2. Effect of the temperature on the extraction of priprioca oil.

4.2 Influence of pressure on the extraction of priprioca oil and black sesame seed oil

In Figs. 3 and 4, it can be seen that an increase in pressure at constant temperature increases the yield and the cumulative amount extracted for both solid matrices studied. The behavior shown in the figures is explained by raising the fluid density that amplifies its solvation power and consequently solubilizes the substances of interest. The proposed model adequately describes the experimental data that show the influence of pressure in the solid matrices.

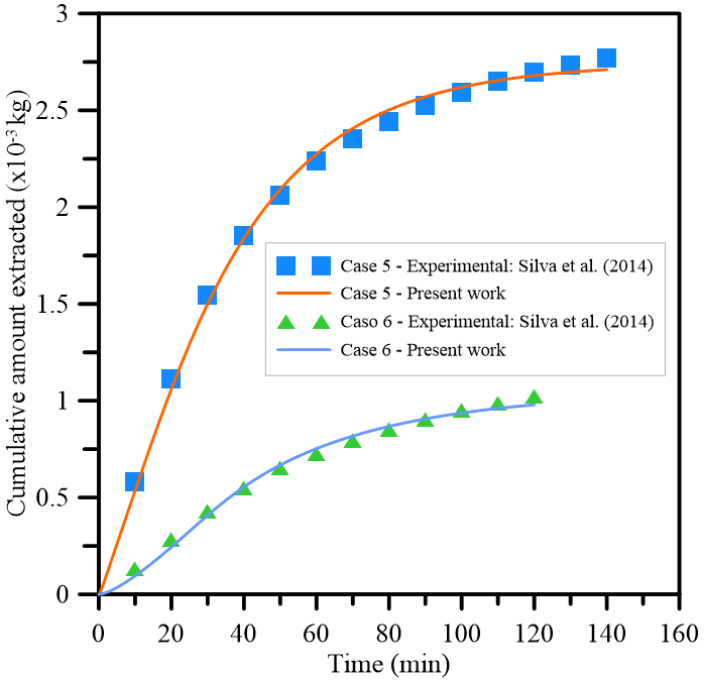

Figure 3. Effect of the pressure on the extraction of priprioca oil.

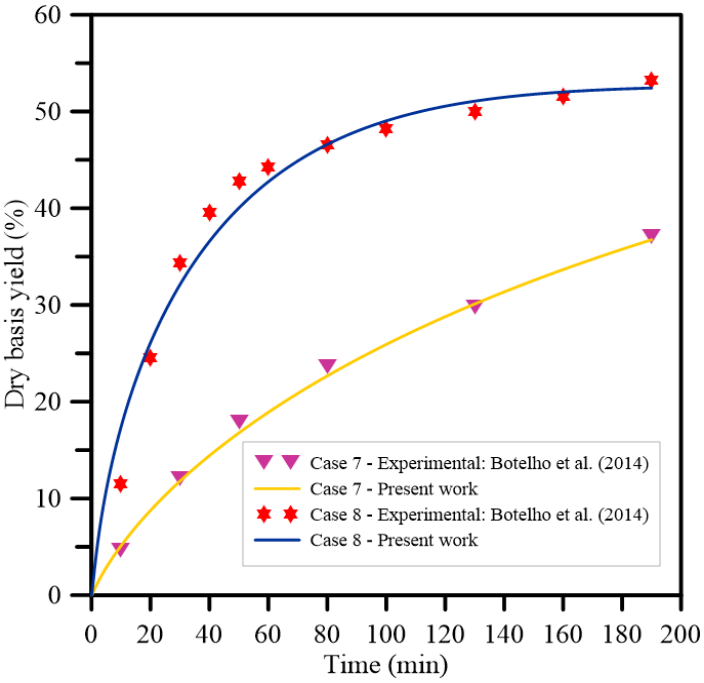

Figure 4. Effect of the pressure on the extraction of black sesame seed oil.

5. CONCLUSION

Mathematical modeling was performed using the equations of species balance. The numerical solutions were obtained using the method of lines (MOL), which proved to be adequate and efficient in the resolution of the partial differential equations (PDEs). The results acquired with the solution of the problem via MOL showed a good agreement with the experimental data and with the physical trends of the extraction, this way warranting that the proposed model can be used in the simulation of different solid matrices in different temperature and pressure conditions.

6. ACKNOWLEDGEMENTS

Conselho Nacional de Desenvolvimento Científico e Tecnológico (CNPq).

7. REFERENCES

Botelho, J.R.S., Medeiros, N.G., Rodrigues, A.M.C., Araújo, M.E., Machado, N.T., Santos, A.G., Santos, I.R., Gomes-Leal, W. and Carvalho Jr., R.N., 2014. "Black sesame (*Sesamum indicum L.*) seeds extracts by CO2 supercritical fluid extraction: isotherms of global yield, kinetics data, total fatty acids, phytosterols and neuroprotective effects". *The Journal of Supercritical Fluids*, Vol. 93, pp. 49-55.

Cordeiro, R.M., Silva, A.P.S., Pinto, R.H.H., Costa, W.A., Silva, S.H.M., Pinheiro, W.B.S., Arruda, M.S.P. and Carvalho Jr., R.N., 2018. "Supercritical CO_2 extraction of ucuúba (Virola surinamensis) seed oil: global yield, kinetic data, fatty acid profile, and antimicrobial activities". *Chemical Engineering Communications*, Vol. 206, pp. 86-97.

Costa, F.M., 2015. *Extração de compostos bioativos de folhas de Vernonia amygdalina Delile utilizando dióxido de carbono em condições supercríticas.* M.Sc. thesis, Universidade Federal de Uberlândia, Uberlândia, Brasil.

Goto, M.; Roy, B. C.; Hirose, T., 1996. "Shrinking-core leaching model for supercritical-fluid extraction". *The Journal Of Supercritical Fluids*, v. 9, n. 2, p. 128-133.

Hernández, S.M.P., Estévez, J.J., Giraldo, L.J.L. and Méndez, C.J.M., 2019. "Supercritical extraction of bioactive compounds from cocoa husk: study of the main parameters". *Revista Facultad de Ingeniería Universidad de Antioquia*, n. 91, pp. 95-105.

Jesus, S.P., 2015. *Modelagem da cinética de transferência de massa no processo de extração supercrítica a partir de produtos naturais*. Ph.D. thesis, Universidade Estadual de Campinas, Campinas, Brasil.

Knez, Ž., Markočič, E., Leitgeb, M., Primožič, M., Hrnčič, M.K. and Škerget, M., 2014. "Industrial applications of supercritical fluids: A review". *Energy*, Vol. 77, pp. 235-243.

Leybros, A., Grandjean, A., Segond, N., Messalier, M. and Boutin, O., 2016. "Cesium removal from contaminated sand by supercritical CO_2 extraction". *Journal of Environmental Chemical Engineering*, Vol. 4, pp. 1076-1080.

Marcus, Y., 2019. "Some advances in supercritical fluid extraction for fuels, bio-materials and purification". *Processes*, Vol. 7, pp. 156-169.

Oliveira, E. L.G. Silvestre, A.J.D.; Silva, C.M., 2011. "Review of kinetic models for supercritical fluid extraction". *Chemical Engineering Research and Design*, v. 89, p. 1104-1117.

Özisik, M.N., Orlande, H.R.B., Colaço, M.J. and Cotta, R.M., 2017. *Finite Difference Methods in Heat Transfer*. CRC Press, Boca Raton, 2nd edition.

Peel, R.G., Benedek, A. and Crowe, C.M., 1981. "A branched pore kinetic model for activated carbon adsorption". *AIChE Journal*, Vol. 27, pp. 26-32.

Reverchon, E.; Donsi, G.; Osseo, L.S., 1993, "Modeling of supercritical fluid extraction from herbaceous matrices". *Industrial & Engineering Chemistry Research*, v. 32, n. 11, p. 2721-2726.

Santos, D.N., 2012. *Extração com dióxido de carbono supercrítico e estudo da composição dos extratos de sementes de Pitanga (Eugenia uniflora L.).* M.Sc. thesis, Universidade de São Paulo, Pirassununga, Brasil.

Santos, J.C., 2011. *Extração com fluido supercrítico e suas aplicações na obtenção de produtos naturais*. Undergraduate thesis, Universidade Federal do Rio Grande do Sul, Porto Alegre, Brasil.

Santos, O.V. and Lannes, S.C.S., 2015. "Application of supercritical fluid extraction technology to obtain Brazil nut oil". In: Lindy, J. (Ed.). *Supercritical fluid extraction: Technology, Application and Limitations*. Nova Science Publishers, New York.

Silva, I.C.M., Santos, W.L., Leal, I.C.R., Zoghbi, M.G.B., Feirhmann, A.C., Cabral, V.F., Macêdo, E.N. and Cardozo-Filho, L., 2014. "Extraction of essential oil from Cyperus articulatus L. var. articulatus (priprioca) with pressurized CO2". *The Journal of Supercritical Fluids*, Vol. 88, pp. 134-141.

Sovová, H., 1994. "Rate of the vegetable oil extraction with supercritical CO2-I. Modelling of extraction curves", *Chemical Engineering Science*, v. 49, p. 409-414.

Tomovic, V., Sojic, B., Jokanovic, M., Skaljac, S. and Pavlic, B., 2019. "Application of essential oil and supercritical fluid extracts in meat processing". *IOP Conference Series: Earth and Environmental Science*, Vol. 333, pp. 012-018.

Tyśkiewicz, K., Konkol, M. and Rój, E., 2018. "The application of supercritical fluid extraction in phenolic compounds isolation from natural plant materials". *Molecules*, Vol. 23, pp. 262-265.

Yao, Y., Farac, N.F. and Azimi, G., 2017. "Supercritical fluid extraction of rare earth elements from nickel metal hydride battery". *ACS Sustainable Chemistry & Engineering*, Vol. 6, pp. 1417-1426.

8. RESPONSIBILITY NOTICE

The authors are the only responsible for the printed material included in this paper.